LIMNOLOGY and OCEANOGRAPHY

ASLO

Limnol. Oceanogr. 67, 2022, 1274–1286

doi: 10.1002/lno.12076

Consequences of an ecosystem state shift for nitrogen cycling in a desert stream

Miquel Ribot [1*], **Nancy B. Grimm** [2], **Lindsey D. Pollard** [2], **Daniel von Schiller** [3], **Amalia M. Handler** [2], **Eugènia Martí** [1]

[1]Integrative Freshwater Ecology Group, Centre d'Estudis Avançats de Blanes (CEAB-CSIC), Blanes, Spain
[2]School of Life Sciences, Arizona State University, Tempe, Arizona
[3]Departament de Biologia Evolutiva, Ecologia i Ciències Ambientals (BEECA), Institut de Recerca de l'Aigua (IdRA), Universitat de Barcelona, Barcelona, Spain

Abstract

Cessation of cattle grazing has resulted in the reestablishment of wetlands in some streams of the U.S. Southwest. Decades of cattle grazing prevented vascular plant growth in Sycamore Creek (Arizona, U.S.A.), resulting in stream reaches dominated by diatoms and filamentous green algae. Establishment of vascular plants can profoundly modify ecosystem processes; yet, the effects on nitrogen (N) cycling remain unexplored. We examined the consequences of this ecosystem state shift on N cycling in this N-limited desert stream. We compared results from whole-reach ammonium-N stable isotope ($^{15}NH_4^+$) tracer additions conducted before (pre-wetland state) and 13 yr after (wetland state) free-range cattle removal from the watershed. Water column estimations showed that in-stream N uptake and storage were higher in the pre-wetland than in the wetland state. N turnover was also higher in the pre-wetland state, indicating that assimilated N was retained for shorter time in stream biomass. In addition, N uptake was mostly driven by assimilatory uptake regardless of the ecosystem state considered. Water column trends were mechanistically explained by the fact that the dominant primary uptake compartments in the pre-wetland state (i.e., algae and diatoms) had higher assimilatory uptake and turnover rates than those in the wetland state (i.e., vascular plants). Overall, results show that the shift in the composition and dominance of primary producers induced by the cessation of cattle grazing within the stream-riparian corridor changes in-stream N processing from a dominance of intense and fast N recycling to a prevalence of N retention in biomass of primary producers.

Ecosystem state shifts refer to changes in ecosystem structure that encompass time scales exceeding the range of natural variability after episodic or abrupt stochastic events, anthropogenic forcing, or due to the ascendance of key species commonly referred as ecosystem engineers. Stochastic events include weather extremes, fires, or pest outbreaks, whereas anthropogenic forcing is associated with land transformation, habitat fragmentation, and climate change (Scheffer et al. 2001; Steffen et al. 2011). Ecosystem engineers refers to organisms, such as several animals (e.g., beavers, salmons, and hippos) with the capacity to physically modify the abiotic environment (Moore 2006; Dutton et al. 2021). The resulting alternative ecosystem states are often characterized by a different physicochemical template and by assemblages of primary producers that differ from the previous ecological community in terms of standing stock, morphologic, and metabolic characteristics (McGowan et al. 2005; Law et al. 2016; Dutton et al. 2021). In addition, the persistence of new assemblages of primary producers is reinforced by positive feedbacks, such as anchoring of sediment by vegetation that prevents scour and removal of that vegetation (Heffernan 2008; Dong et al. 2016). Consequences of ecosystem state shifts have mainly been described in marine and terrestrial ecosystems, such as coral reefs, rocky macroalgal communities, woodlands, deserts, and lakes (Scheffer et al. 2001; Conversi et al. 2015; Boada et al. 2017); less so in streams and rivers (but see Ibáñez et al. 2012; Brighenti et al. 2019).

A decade ago, Heffernan and co-authors documented an ecosystem state shift in a desert stream in the U.S. Southwest

*Correspondence: mribot@ceab.csic.es

Author Contribution Statement: E.M., N.B.G., M.R., and D.v.S. contributed to the study's conception and development. E.M., N.B.G., M.R., and L.D.P. conducted fieldwork and data acquisition with assistance from A.M.H. E.M., M.R., and L.D.P. conducted laboratory and data analysis. M.R. and E.M. wrote the manuscript with substantial contributions from L.D.P., D.v.S., A.M.H., and N.B.G. All authors approved the final submitted manuscript.

that corresponded to a change in the watershed management practices (Heffernan 2008; Heffernan et al. 2008). Cattle removal from the watershed, per an agreement between the U.S. Forest Service and the ranchers, was instigated by a shift in federal grazing policy in western United States as a result of the cessation of cattle grazing along the stream-riparian corridor, stream reaches dominated by algae on gravel substrata to a state with abundant emergent vascular plants, which slowed water flow rates and promoted wetland conditions within the stream channel. The resulting wetlands represent an alternative stable state of desert streams (Heffernan 2008). This ecosystem state shift and changes associated with it have since been intensively investigated in Sycamore Creek (Heffernan et al. 2008; Dong et al. 2016, 2017).

Prior to cattle removal, high light levels reaching the stream bottom supported high rates of algal production (Busch and Fisher 1981; Grimm 1987). Under baseflow conditions, blooms of filamentous green algae were typical (Fisher et al. 1982; Grimm 1987), and patches of vascular plants were present but rare and limited in spatial extent (Dudley and Grimm 1994). The cessation of cattle grazing in the stream-riparian zone caused an increase in the abundance of vascular plants in many areas of the stream channel, which came to cover a remarkable portion (up to 45%) of the main stem of Sycamore Creek, with > 80% vascular plant cover in some reaches (Dong et al. 2016, 2019). Wetland establishment drives changes in the physical, chemical, and biological structure of desert streams, reducing surface-flow velocity and water exchange between the surface and subsurface, increasing standing crops of live biomass and organic detritus, and increasing spatial heterogeneity (Heffernan 2008; Heffernan et al. 2008; Dong et al. 2017).

A shift in dominance of algae to vascular plants is also expected to strongly affect stream ecosystem processes, including nutrient cycling (Twilley et al. 1985; Levi et al. 2015; Riis et al. 2019). This effect may be especially relevant for nitrogen (N) cycling in desert streams of the U.S. Southwest because this element is the limiting nutrient for in-stream biota in these ecosystems (Grimm and Fisher 1986; Peterson and Grimm 1992). Uptake of N in streams is primarily driven by benthic organisms, which have recently been referred to as primary uptake compartments (PUCs) because they meet their N demand via direct uptake of N from the water column (Tank et al. 2018). Biotic compartments of N uptake include both autotrophic microorganisms (i.e., epilithic biofilm dominated by microalgae, filamentous green algae, vascular plants, and bryophytes) and heterotrophic microorganisms (i.e., bacteria and fungi in biofilms on fine benthic organic matter [FBOM], decomposing leaves, and wood). Autotrophs show large variation in nutrient uptake and turnover rates (Mulholland et al. 2000; Peipoch et al. 2014), and among them, vascular plants tend to have higher nutrient and energy requirements than filamentous algae or single-celled organisms such as diatoms (Dodds et al. 2004; Allen et al. 2005). Therefore, the shift in the dominant primary producers within the stream associated with cattle removal may directly affect N cycling at the reach scale. In addition, the development of vascular plants in the stream channel may indirectly affect N cycling via changes in stream hydromorphology. For instance, the reduction of water exchange between surface and subsurface water associated with plant establishment may decrease the contribution of the hyporheic zone, a key N retention compartment, on in-stream N uptake (Hall et al. 2002; Wollheim et al. 2014; Drummond et al. 2016). Conversely, the presence of plants may also increase water residence time within the stream channel, which may enhance N retention (Salehin et al. 2003; Nikolakopoulou et al. 2018).

Here, we aimed to examine how changes in the composition and dominance of primary producers caused by the ecosystem state shift in desert streams affected in-stream N cycling. We compared results from whole-reach ^{15}N stable isotope tracer additions conducted before and after free-range cattle removal from the Sycamore Creek watershed. Specifically, we assessed changes in N cycling processes between a stream reach in pre-wetland state (i.e., dominated by filamentous green algae and diatoms) sampled in 1997, and a stream reach in wetland state (i.e., extensively colonized by emergent vascular plants) sampled in 2013. We hypothesized that differences in the structural and metabolic characteristics of the dominant primary producers between the two ecosystem states would be reflected in contrasting N cycling at the reach scale. Specifically, we predicted (1) lower N uptake and storage in the pre-wetland state, because algae and bacteria have smaller assimilative requirements for biomass than vascular plants and (2) higher N turnover in the pre-wetland state, because algae and bacteria have higher growth rates but shorter lifespans than vascular plants.

Materials

Study site and sampling design

Sycamore Creek is a ~ 65-km-long desert stream located in the Sonoran Desert (32 km NE of Phoenix, Arizona, U.S.A.), which drains a 505 km^2 watershed of mountainous terrain where elevation ranges from 427 to 2164 m. Annual precipitation (average between 7 and 43 cm) occurs during the monsoon season (July–September), producing intense, isolated rainfall and flash flooding, and during winter (January–March), when rain and flooding are more prolonged (Schade et al. 2005). This precipitation seasonality coupled with high interannual variability in rainfall results in a disturbance regime that exhibits widely varying frequency, intensity, and timing of flash floods (Grimm and Fisher 1989). The hydrological regime greatly affects the temporal dynamics of stream ecosystem structure and function, the morphology of the stream channel, and the temporal variation in nutrient concentrations. The stream base flow (i.e., ~ 100 and ~ 10 L s^{-1} in winter and summer, respectively) may increase by as much as

4–5 orders of magnitude during flash floods, which maintains an active channel that is much wider than the wetted stream and light availability is usually not a limiting factor for development of photoautotrophs (Peterson and Grimm 1992). Concentration of dissolved inorganic nitrogen (DIN) is consistently very low (< 10 μg L^{-1}) throughout the year, except during floods. Availability of N has been shown to be a limiting factor for the communities and the ecosystem function of this stream (Grimm and Fisher 1986).

The tracer additions of N stable isotope in 1997 and 2013 were conducted in the middle reaches of Sycamore Creek (between 610 [1997] and 690 [2013] m elevation; UTM: 3732592N, 451899E and 3732557N, 451947E, respectively), where shifts in ecosystem state have been remarkable (Fig. 1). Wetland expansion began in the year 2000, initially with aquatic vascular plants such as *Veronica* spp. and *Nasturtium officianale* and the grass, *Paspalum distichum* (Heffernan 2008), later giving way to extensive stands of cattail, *Typha* spp. and bulrush, *Schoenoplectus americanus* (Dong et al. 2016). Wetland reaches are concentrated near locations of high water permanence (Dong et al. 2016, 2017), which included the two sites selected for this study. Although wetland vegetation was present at both sites in 2013, the more downstream site (used in 1997) had a much wider channel owing to extensive flooding in 2010, and the wetlands did not extend across the channel. Furthermore, because Sycamore Creek has experienced overall flow reductions during the current decades-long drought in the U.S. Southwest, there was a risk that the 1997 (downstream) site would dry before we could complete the experiment. Thus, we opted to conduct the tracer additions in the upstream site, which supported bank-to-bank cover of *S. americanus*, to maximize the differences in wetland cover between the two experiments.

In the pre-wetland state, the addition was done in a 180-m open reach where the wetted channel was dominated by diatoms and filamentous green algae (Chlorophyta), such as *Cladophora glomerata* and Zygnematales (*Zygnema* spp. and *Spirogyra* spp.) In the wetland state, the addition was done in the upstream reach (170 m long), where the wetted channel was dominated by riverine aquatic emergent vascular plants (mainly *S. americanus* and *Typha domingensis*, with some *P. distichum*). Mature willows (*Salix goodingii*) and cottonwoods (*Populus fremontii*) dominated the areas immediately lateral to the wetted channel, providing some shade throughout the growing season (February–July). The stable isotope additions started on 01 May 1997 and 04 June 2013 for the pre-wetland and wetland states, respectively. Both additions were done under base flow conditions and after more than 1 month since the last flood, thus the in-stream communities were well developed and representative of each ecosystem state.

Field methods

To assess N cycling at the reach scale and the role of different primary producers under the two alternative states, we conducted constant-rate additions of ^{15}N (as $^{15}NH_4^+$) for seven consecutive days in each reach. To determine the most abundant PUCs in the pre-wetland and wetland state stream reaches, we measured the percent coverage of each PUC in the reach. We defined 6–8 cross-sectional transects as sampling stations, which were evenly distributed along each study reach. In addition, we defined one sampling station upstream from the addition points used as reference for background conditions. In the wetland state reach, we installed four PVC piezometers (internal diameter: 2.5 cm) in the stream thalweg at 20, 45, and 60 m downstream and 5 m upstream of the addition point to collect samples of subsurface water. Piezometers reached a depth of ~ 25 cm below the sediment surface.

Prior to the start of the $^{15}NH_4^+$ addition, we collected samples of surface and subsurface water at the sampling stations to measure ambient water chemistry, electrical conductivity (EC), and $\delta^{15}N$ signatures of NH_4^+ and NO_3^-. To collect subsurface water, we purged the piezometers twice before taking

Fig. 1. General view of the pre-wetland and wetland state reaches where the $^{15}NH_4^+$ additions were conducted in 1997 and 2013, respectively.

the sample with a 100-mL syringe connected to silicone tubing inserted into the piezometer. We also collected samples from the most abundant PUCs at each station to estimate N standing stocks (mg N m^{-2}) and background $\delta^{15}N$ signatures. In the case of vascular plants, at each station we collected samples of aboveground (i.e., stem and leaves separately) and belowground (i.e., roots) biomass to estimate $\delta^{15}N$ signatures. We repeated the sampling of water and PUCs for nutrient chemistry and isotopic ^{15}N signatures at the same stations after 7 d, under conditions when the ^{15}N tracer addition had reached plateau along the reach, as verified with a conservative tracer (bromide; *see* below). We filtered all water samples in the field through ashed Whatman (Maidstone, U.K.) GF/F glass-fiber filters. We stored the filtrate on ice in the field and kept it frozen in the laboratory until further processing and analysis. We stored samples for PUCs in plastic bags and brought them to the laboratory for further processing.

We sampled the following PUCs in the pre-wetland state reach: periphyton developed on fine gravel (predominantly diatoms), filamentous green algae (*C. glomerata* and Zygnematales), cyanobacteria (*Nostoc* spp.), and FBOM; and the following PUCs in the wetland state reach: periphyton developed on cobbles (predominantly diatoms), *S. americanus*, *T. domingensis*, FBOM, and submerged roots in the stream channel from *S. goodingii* growing on the stream margins.

We sampled periphyton on fine gravel, filamentous green algae, and cyanobacteria using a 24.6-cm^2 core. We collected periphyton on cobbles by scraping randomly collected rocks and filtering the slurry onto ashed and pre-weighed Whatman GF/A glass-fiber filters. We estimated cobble surface area by tracing the rock onto weighing paper and calculating the surface area compared to a known area of weighing paper. We sampled FBOM using a syringe to collect an aliquot of the material suspended by manual agitation of a known water volume contained in a plastic corer of 78.5 cm^2. We filtered the FBOM aliquot onto ashed and pre-weighed Whatman GF/F glass-fiber filters. We sampled submerged willow roots by collecting all material found within a quadrat of 81 cm^2. For vascular plants, we used a nondestructive approach to estimate the mean aboveground biomass for each wetland species. We averaged percent cover, stem width, and stem length throughout the entire reach (area = total reach length × average reach width). We then applied established species-specific height-to-dry mass (DM) relationships to estimate total reach biomass (N. B. Grimm unpubl.). We estimated the belowground biomass of vascular plants using the above-to-belowground biomass ratio of a study conducted in a constructed treatment wetland located ~ 80 km from the Sycamore watershed, which included the same wetland species (Weller et al. 2016). Despite different nutrient conditions, previous studies suggest that the availability of nutrients has a low effect on the above-to-belowground biomass ratio on different wetland species of the same genus (Svengsouk and Mitsch 2001; Kearney and Zhu 2012).

Once background samples were collected, we added at the head of the reach a solution containing $^{15}NH_4^+$ in the form of either $^{15}NH_4Cl$ (in 1997) or $(^{15}NH_4)_2\ SO_4$ (in 2013) and bromide as a conservative tracer in the form of NaBr. We added the enriched solution at a constant rate using a battery-powered Fluid Metering peristaltic pump. To achieve a target $\delta^{15}N$ enrichment of 1000‰ in the water column, we calculated the appropriate concentration of $^{15}NH_4^+$ based on stream discharge. To verify plateau conditions along the reach during the $^{15}NH_4^+$ addition, we collected water samples at each sampling station 1 d before and at days 1, 3, and 7 after the starting of the ^{15}N tracer addition to measure Br- concentration. We used longitudinal changes in Br- concentration at plateau to calculate the percentage of dilution along the reach as an estimate of the lateral inflow from subsurface water. During each addition, we also measured hydraulic parameters such as discharge and water velocity by conducting slug additions of diluted NaCl (Gordon et al. 2004) on four separate days (i.e., −1, 3, and 7 d after the starting of the ^{15}N tracer addition). We measured EC using a Yellow Springs Instruments conductivity meter. The $^{15}NH_4^+$ tracer additions only slightly increased background NH_4^+ concentrations (i.e., 0.2% and 3.2% in the pre-wetland and wetland state, respectively).

In the pre-wetland (1997) experiment, we measured dissolved oxygen (DO) concentration and water temperature at hourly intervals at the end of the reach using the Winkler titration method (APHA 1995) over 24 h. In the wetland (2013) experiment, we recorded DO concentration and percentage saturation, and water temperature at the end of the reach at 15-min intervals over four 24-h periods using a Yellow Springs Instruments model 556 multiparameter sonde (sensor accuracy: ± 2% of the reading, resolution: 0.02 mg L^{-1}, and calibrated prior its use following manufacturer's instructions). We used these data to estimate reach-scale metabolism using the open-system, single-station approach (Hall and Hotchkiss 2017). We calculated daily rates of gross primary production (GPP) and ecosystem respiration (ER) by integrating the DO fluxes (corrected for reaeration) estimated at the bottom of the reach over 24 h. Reaeration coefficients (K_{oxy}) estimated with the nighttime regression method (Kosinski 1984) were 19.6 d^{-1} and 10.5 ± 0.2 d^{-1} (mean ± SE) for pre-wetland and wetland state, respectively. The reach lengths associated with the turnover of DO along the stream, estimated from Hall and Hotchkiss (2017), were 3.8 and 5.8 km for pre-wetland and wetland state, respectively. We extrapolated instantaneous respiration rates at night to 24 h to estimate ER. We multiplied daily rates of GPP and ER by the mean water column depth in the reach to obtain areal estimates.

Laboratory methods

In the pre-wetland state, we analyzed concentrations of NO_3^- and soluble reactive phosphorus (SRP) on a Bran and Luebbe TRAACS® 800 autoanalyzer. We manually analyzed

NH_4^+ concentration using the phenolhypochlorite colorimetric method (Solórzano 1969). In the wetland state, we analyzed NO_3^-, NH_4^+, and SRP concentrations using flow-injection analysis (Lachat QC8000). We analyzed dissolved organic carbon (DOC) and total dissolved nitrogen (TDN) using a total organic carbon/nitrogen analyzer (Shimadzu TOV-C). We calculated dissolved organic N (DON) by subtracting DIN (calculated as $NO_3^- + NH_4^+$) from TDN. We analyzed bromide concentrations on grab water samples using ion chromatography (Dionex ICS 2000). We reported all nutrient concentrations in units of elemental mass/volume (e.g., mg N L^{-1}).

We determined isotopic enrichment of $^{15}NH_4^+$ in stream water using the ammonia-diffusion procedure (Holmes et al. 1998). We used the same procedure for isotopic enrichment of $^{15}NO_3^-$ after reduction of $^{15}NO_3^-$ to $^{15}NH_4^+$ with Devarda's alloy (Sigman et al. 1997). Due to the low ambient concentrations of NH_4^+ and NO_3^- in Sycamore Creek, we spiked the $^{15}NH_4^+$ and $^{15}NO_3^-$ samples with 200 μL of a standard solution of 100 ppm $(NH_4)_2$ SO_4 and KNO_3, respectively, to bring the total N mass to the minimum required for detection by the mass spectrometer (i.e., 17 μg N). Isotopic enrichment is expressed in delta values (δ):

$$\delta^{15}N(‰) = \left[\left(R_{sample}/R_{standard}\right) - 1\right] \times 1000 \quad (1)$$

where R_{sample} is the $^{15}N : {}^{14}N$ ratio in the sample and $R_{standard}$ is the $^{15}N : {}^{14}N$ ratio in atmospheric N_2 ($R_{standard} = 0.0036765$).

We measured patch-specific DM (mg) of each PUC by oven drying the samples at 60°C to constant weight, then weighing to the nearest 0.1 mg. We estimated the total DM of each PUC in the reach using the patch-specific DM and its percent cover. We divided this DM by the surface area of the reach (length × average width) to estimate reach-scale DM (mg m^{-2}) of each PUC. We estimated reach-scale N standing stocks (mg N m^{-2}) for each PUC by multiplying the reach-scale DM standing stock by the percentage of N in DM.

We prepared PUC pre- and plateau-addition samples for ^{15}N analysis by oven drying at 60°C to constant weight, and then processing dried samples according to specific isotope facility protocols. $^{15}NO_3^-$, $^{15}NH_4^+$, and PUC samples were analyzed at the University of California Stable Isotope Facility (Davis, California, U.S.A.). The N content (as a percent of DM) and stable isotope ratios were measured by continuous flow isotope-ratio mass spectrometry (20–20 mass spectrometer; PDZEuropa, Northwich, U.K.) after sample combustion in an on-line elemental analyzer (PDZEuropa ANCA-GSL).

Calculation of N uptake metrics

We calculated reach-scale and PUC-specific N uptake parameters following the procedures described in Mulholland et al. (2000) and Tank et al. (2018). We calculated the surface water ^{15}N-NH_4^+ flux at each station by multiplying background-corrected $\delta^{15}NH_4^+$ signatures at plateau 7 d by the station-specific discharge estimated based on the Br- dilution along the reach during plateau. We estimated the uptake rate per unit distance (k_w, m^{-1}) in the reach from the slope of the regression of the ln-transformed tracer ^{15}N fluxes vs. site distance from the top of the reach. We calculated the uptake length (S_w, m) as the inverse of k_W and converted it to uptake velocity (V_f; mm min^{-1}) by dividing the stream-specific discharge (i.e., discharge/wetted width) by S_w (Stream Solute Workshop 1990). We calculated the areal uptake (U; μg N m^{-2} s^{-1}) by multiplying V_f by the mean ambient NH_4^+ concentration. We calculated the uncertainty for each nutrient retention metric (i.e., S_w, V_f, and U) by first running Monte Carlo simulations (n = 10,000) based on the mean and the standard deviation (SD) of each parameter used (i.e., discharge, k_w, NH_4^+ concentration, and wetted width). Then, we recalculated each retention metric but substituting the parameters by their simulations. The resulting SD was reported as uncertainty.

We estimated the fractional uptake rate per unit distance for nitrification (k_{NIT}) by fitting the $^{15}NO_3^-$ tracer fluxes vs. distance to a two-box model as proposed by Mulholland et al. (2000) using a nonlinear regression model with two unknown parameters (i.e., k_2 as $^{15}NO_3^-$ uptake rate and k_{NIT}). We calculated the reach-scale areal uptake for nitrification (U_{NIT}, μg N m^{-2} s^{-1}) from k_{NIT}, as previously described for U. We calculated the uncertainty for U_{NIT} by first running Monte Carlo simulations (n = 10,000) based on the mean and SD of each parameter used (i.e., discharge, k_{NIT}, NH_4^+ water concentration, and wetted width). Then, we recalculated U_{NIT} but substituting the parameters by their simulations. The resulting SD was reported as uncertainty. Furthermore, we calculated the reach-scale assimilatory uptake ($U_{ASSIM-WATER}$, μg N m^{-2} s^{-1}) by subtracting U_{NIT} from U. Finally, we calculated the uncertainty for $U_{ASSIM-WATER}$ by running Monte Carlo simulations (n = 10,000) with the mean and SD values of each parameter and by using the same equation but with the simulation results. The resulting SD was reported as uncertainty.

To estimate the PUC-specific NH_4^+ assimilatory uptake of periphyton, filamentous green algae, Cyanobacteria, and FBOM, we divided the reach-weighted mass of background-corrected ^{15}N tracer per m^2 measured in each biotic compartment by the total ^{15}N addition time in seconds and the fraction of ^{15}N in the stream surface water flux of NH_4^+. To estimate NH_4^+ assimilatory uptake of vascular plants, we used the same calculation approach but considering ^{15}N-NH_4^+ in the subsurface water. In addition, we calculated separately NH_4^+ assimilatory uptake from aboveground (sum of stem and leaves) and belowground (roots) biomass to infer where assimilated N was stored in vascular plants. For this calculation, we only considered data from the two uppermost sampling stations downstream of the addition point (i.e., 25 and 40 m, respectively) to avoid confounding effects of N regeneration along the reach. We then estimated the areal NH_4^+

assimilatory uptake by PUCs at the reach scale ($U_{ASSIM-PUC}$, μg N m^{-2} s^{-1}) as the sum of the mean compartment-specific NH_4^+ assimilatory uptake of each PUC. We calculated the uncertainty for $U_{ASSIM-PUC}$ by running Monte Carlo simulations (n = 10,000) with the mean and SD values of each PUC U_{ASSIM} and then summing up U_{ASSIM} simulations of each PUC. The resulting SD was reported as uncertainty.

For each PUC, we also calculated the biomass-specific N uptake (mg N mg N^{-1} d^{-1}), a surrogate of N turnover rate, by dividing PUC-specific NH_4^+ assimilatory uptake by the N content in PUC biomass (Dodds et al. 2004). Likewise, we estimated the biomass-specific N uptake (mg N mg N^{-1} d^{-1}) at reach scale, a surrogate of N turnover rate for each stream reach, as $U_{ASSIM-PUC}$ divided by the sum of the N content in all PUCs. We calculated the uncertainty for biomass-specific N uptake at reach scale by substituting the parameters in the equation by their corresponding simulations computed with the Monte Carlo method (n = 10,000 runs). The resulting SD was reported as uncertainty.

We calculated reach-scale N storage in the PUCs as the percentage of ^{15}N added during the addition that was estimated in the biomass of the different PUCs at the addition plateau. For each PUC, the total mass of stored ^{15}N was based on an integration of the downstream decline in compartment-specific ^{15}N-biomass along the reach. If the slope of the regression of ^{15}N biomass vs. distance was not significant ($p > 0.05$), we used the mean ^{15}N biomass for the entire reach. For this calculation, we used a reach length equal to five times the measured S_w to standardize estimates for variable reach lengths across the pre-wetland and wetland reaches. This standardization ensured that > 99% of the ^{15}N tracer was removed; so our calculations fully encompass the reach length where biota was exposed to $^{15}NH_4^+$ from the water column (Mulholland et al. 2000). We performed the computations in R version 1.4.1106 (R Core Team 2018). Statistical results were evaluated at the $\alpha = 0.05$ significance level.

Results

Environmental characteristics of surface water in the two alternative states

The pre-wetland state reach was wider and shallower than the wetland state and had a higher discharge throughout the ^{15}N tracer additions (Table 1). Results of NaCl additions from day −1 and day 7 indicated that discharge decreased by 15% and 27% in the pre-wetland and wetland state reaches, respectively, due to extreme weather conditions. Dilution factors along the two reaches calculated from longitudinal patterns of bromide concentrations at plateau on day 7 were 5% and 1% for pre-wetland and wetland state, respectively. The two reaches had similar water temperature, whereas EC was lower in the pre-wetland state and concentration of DO was higher in the pre-wetland state (Table 1). Ambient NO_3^- and NH_4^+ concentrations were similarly low between the two study reaches (Table 1). Concentration of DON was an order of magnitude higher than that of DIN and similar between stream states (Table 1). Concentration of SRP was four times lower in the pre-wetland state; however, low DIN : SRP ratios (< 3) indicated potential N limitation in the two study states (Table 1). Concentration of DOC was slightly lower in the pre-wetland state reach (Table 1). The daily GPP rate was higher in the pre-wetland state, and ER was similar in both states. Thus, GPP : ER ratio shifted from 1 in the pre-wetland state to < 1 in the wetland state, indicating a more heterotrophic system in the latter state. It is worth noting that the open-channel method used to measure metabolism relies on water-column changes in DO concentration and cannot adequately estimate the photosynthesis and respiration rates of emergent vascular plants. Therefore, these results reflect only the metabolic activity associated with submersed benthic organisms and we

Table 1. Physicochemical characteristics and daily rates of reach-scale metabolism for the pre-wetland and wetland state study reaches during the two $^{15}NH_4^+$ additions. Data for physical parameters (except temperature) are the mean (± standard error; SE) of the four NaCl additions conducted during each addition period. Data for water temperature and DO are the mean (± SE) of the 24-h records used to infer metabolism. Data for EC and nutrient concentrations are the mean (± SE) from samples collected at the different sampling stations along the study reaches at the pre-sampling and the 7-d plateau, respectively. Daily rates of reach-scale GPP and ER were estimated on a single date on the pre-wetland addition and on four dates (mean ± SE) on the wetland addition.

	Pre-wetland	Wetland
Physical		
Discharge (L s^{-1})	43.0±1.5	19.0±2.0
Velocity (cm s^{-1})	28.6±4.8	23.5±5.9
Width (m)	5.8±0.2	2.5±0.3
Depth (cm)	8.3±3	17.1±4.4
Temperature (°C)	23.5±0.6	23.5±0.3
Chemical		
EC (μS cm^{-1})	445±1	601±0.1
DO (mg L^{-1})	8.7±0.7	7.4±0.1
NO_3^- (μg N L^{-1})	9±1	10±1.2
NH_4^+ (μg N L^{-1})	6±1	6±0.8
SRP (μg P L^{-1})	14±0.8	63±1.3
DIN : SRP (molar)	2.3±0.1	0.3±0.09
DON (μg N L^{-1})	179±10	156±4.5
DOC (mg L^{-1})	3.7±0.1	4.7±0.2
Metabolism		
GPP (g O_2 m^{-2} d^{-1})	2.5	0.7±0.02
ER (g O_2 m^{-2} d^{-1})	2.5	2.0±0.2
GPP : ER	1.0	0.33±0.04

cannot draw conclusions about total system production or respiration.

Biomass standing stocks of PUCs in the two alternative states

The total N biomass in PUCs was lower in the pre-wetland reach than in the wetland reach: 4750 (1190) and 7813 (1689) mg N m^{-2}, respectively (mean and SD value based on Monte Carlo method). However, the type and relative contribution of the PUCs to total N biomass clearly differed between the two states (Fig. 2A). In the pre-wetland state, algae and detrital compartments accounted for the majority of reach-scale N biomass. In particular, *C. glomerata* (36.1%) and FBOM (26.1%) contributed the most to the total N biomass, followed by periphyton (18.9%), Zygnematales (10.5%), and *Nostoc* spp. (8.4%). In the wetland state reach, the N biomass at the reach scale was dominated by emergent vascular plants, particularly *S. americanus*, accounting for 78.3% of N biomass, of which 58% was accumulated in belowground biomass (Fig. 3A). The other PUCs contributing to reach-scale N biomass in the wetland state were roots from riparian *S. goodingii* (15.5%), periphyton (3.1%), and FBOM (2.5%). *T. domingensis* accounted for the remaining 0.6% of N biomass in the reach, mostly accumulated in aboveground biomass (Fig. 3A).

N uptake in the two alternative states

In the pre-wetland state, S_w was two times shorter, V_f was one order of magnitude higher, and U was 2.5 times higher than in the wetland state, indicating that the pre-wetland state was more efficient in retaining N and had a higher N uptake capacity (Table 2). Nitrification (U_{NIT}) accounted for 25.2% of U in the pre-wetland state. In the wetland state, U_{NIT} was nil since no significant increase of $^{15}NO_3^-$ was detected along the reach during the ^{15}N addition. Therefore, in the two study reaches, U at the reach scale was dominated by assimilatory uptake ($U_{ASSIM-WATER}$; Table 2).

The sum of assimilatory uptake by PUCs ($U_{ASSIM-PUC}$) at the reach scale was three- to fourfold higher than that measured from the water column (i.e., $U_{ASSIM-WATER}$) in both study reaches. In addition, in the pre-wetland state, $U_{ASSIM-PUC}$ was twofold higher than in the wetland state (Table 2). The relative contribution of each PUC to $U_{ASSIM-PUC}$ varied between the two state reaches (Fig. 2B). In the pre-wetland reach, *C. glomerata* was the PUC with the highest N demand, accounting for 41.8% of $U_{ASSIM-PUC}$, followed by periphyton (22.8%) and Zygnematales (20.5%). The contribution of *Nostoc* spp. and FBOM to $U_{ASSIM-PUC}$ was similar (7.5% and 7.3%, respectively). In the wetland reach, willow roots and *S. americanus* showed the highest contribution to $U_{ASSIM-PUC}$, accounting for 85% of $U_{ASSIM-PUC}$. Periphyton and FBOM accounted for 10.7% and 4.1% of $U_{ASSIM-PUC}$, respectively, whereas *T. domingensis* accounted for only 0.2%.

The portion of added ^{15}N stored in PUCs along the reach differed between the two stream states (Table 2; Fig. 2C). In

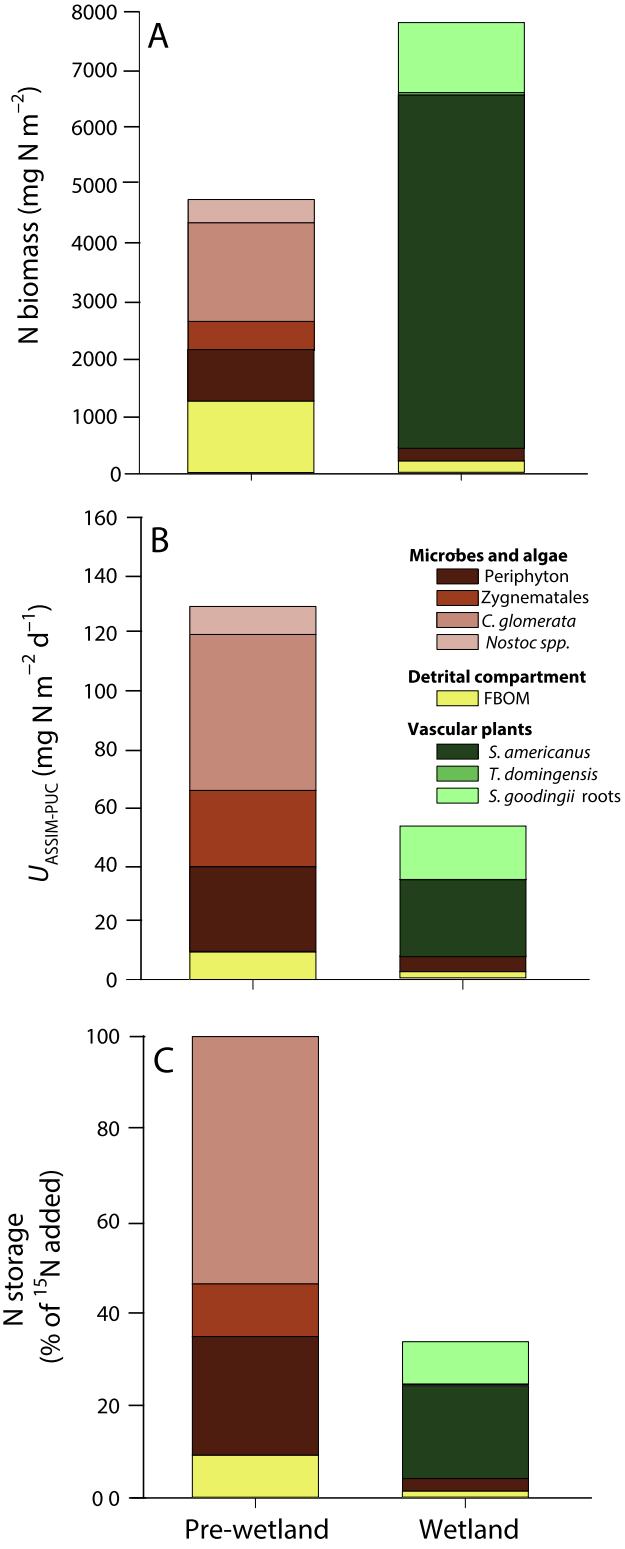

Fig. 2. Reach-scale N biomass (**A**), assimilatory NH_4^+ uptake ($U_{ASSIM-PUC}$) (**B**), and N storage as percentage of total added ^{15}N (**C**) in each of the two study reaches (pre-wetland and wetland state). Different fill in each bar represents the relative contribution of PUCs to reach-scaled totals. FBOM refers to fine benthic organic matter. For clarity, we separated PUCs in three different classes: microbes and algae, FBOM, and vascular plants.

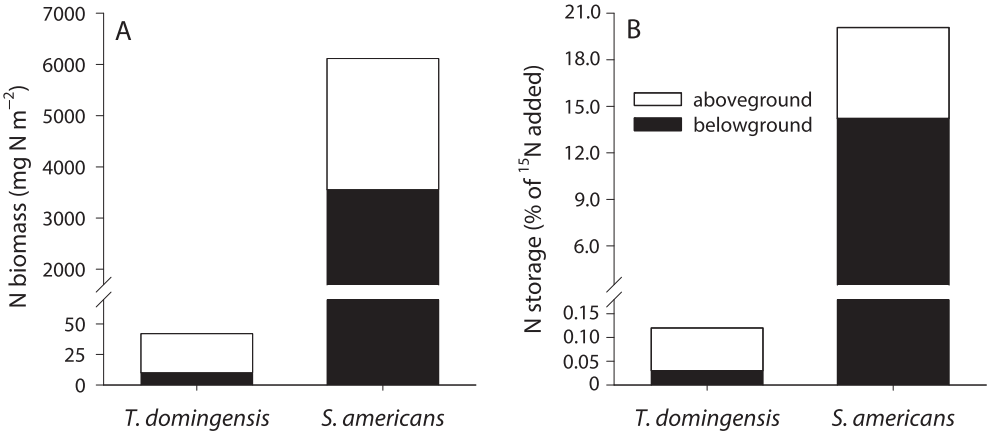

Fig. 3. Reach-scale values for N biomass (**A**) and N storage as a percentage of total added ^{15}N (**B**) for the two most abundant vascular plant species in the wetland state. Different fill in each bar represents the relative contribution of the aboveground and belowground biomass to reach-scaled totals.

the pre-wetland reach, 100% of the ^{15}N added was stored in the sampled PUCs, whereas in the wetland reach, only 33.5% of the ^{15}N added was stored in the sampled PUCs (Table 2). In addition, the relative contribution of each PUC to N storage also differed between the study state reaches (Fig. 2C). In the pre-wetland reach, 53.6% of the total ^{15}N stored was found in *C. glomerata*, followed by periphyton and Zygnematales (24.7% and 11.0%, respectively). *Nostoc* spp. and FBOM stored 2.0% and 9.1%, respectively. In the wetland reach, most N storage occurred in *S. americanus* (59.9%) and in *S. goodingii* roots (27.2%). Periphyton (8.5%), FBOM (4.0%), and *T. domingensis* (0.4%) accounted for the remaining ^{15}N stored (Fig. 2C). Regarding the location of N stored in vascular plants, 71.1% of total ^{15}N assimilated by *S. americanus* was stored in belowground biomass, whereas in *T. domingensis*, N was mostly stored in aboveground biomass (78.3%; Fig. 3B).

The reach-scale N turnover rate was four times higher in the pre-wetland state than in the wetland state (0.03 and 0.007 mg N mg N^{-1} d^{-1}, respectively; Table 2). Within each state, the N turnover rate varied considerably among PUCs (Fig. 4). Filamentous green algae (*C. glomerata* and Zygnematales) and periphyton showed the highest N turnover rates, and the two vascular plants had the lowest rates (Fig. 4). Turnover rates of periphyton and FBOM were similar for the two states.

Table 2. Reach-scale N cycling parameters calculated from the $^{15}NH_4^+$ additions in the pre-wetland and wetland state study reaches. Uncertainty is shown in brackets as the standard deviation calculated based on the Monte Carlo method (see main text for details). n.d. = not detectable.

	Pre-wetland	Wetland
Total NH_4^+ uptake		
S_w (m)	47 (28)	88 (80)
V_f (mm min^{-1})	15.3 (4.2)	1.95 (1.4)
U (μg N m^{-2} s^{-1})	0.48 (0.33)	0.20 (0.19)
Nitrification		
U_{NIT} (μg N m^{-2} s^{-1})	0.12 (0.13)	n.d.
% of the total NH_4^+ uptake	25.2	n.d.
Assimilatory NH_4^+ uptake		
$U_{ASSIM-WATER}$ (μg N m^{-2} s^{-1})	0.36 (0.29)	0.20 (0.19)
$U_{ASSIM-PUC}$ (μg N m^{-2} s^{-1})	1.50 (0.20)	0.62 (0.08)
N storage		
Portion of ^{15}N added (%)	100	33.5
N turnover		
mg N mg N^{-1} d^{-1}	0.03 (0.02)	0.007 (0.002)

Discussion

We compared N uptake, storage, and turnover, derived from ^{15}N-NH_4^+ tracer additions, between two stream reaches representative of two alternative ecosystem states in Sycamore Creek, a desert stream in Arizona, U.S.A. (Fig. 1). The reach in the pre-wetland state was characterized by a gravel-bed reach dominated by Chlorophyta and microbial

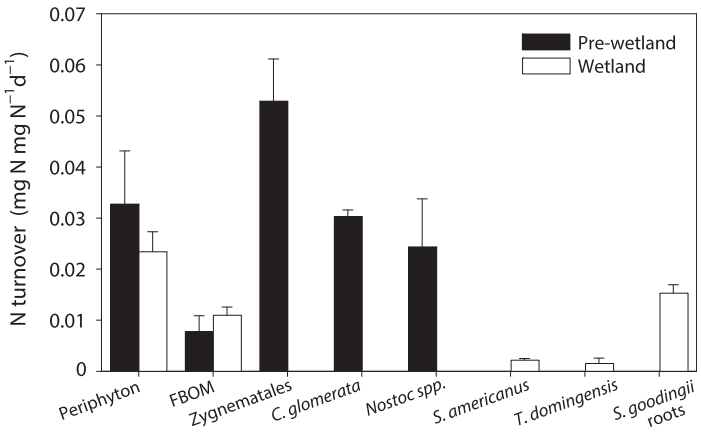

Fig. 4. N turnover rate of the different PUCs in each of the two study reaches (pre-wetland and wetland state).

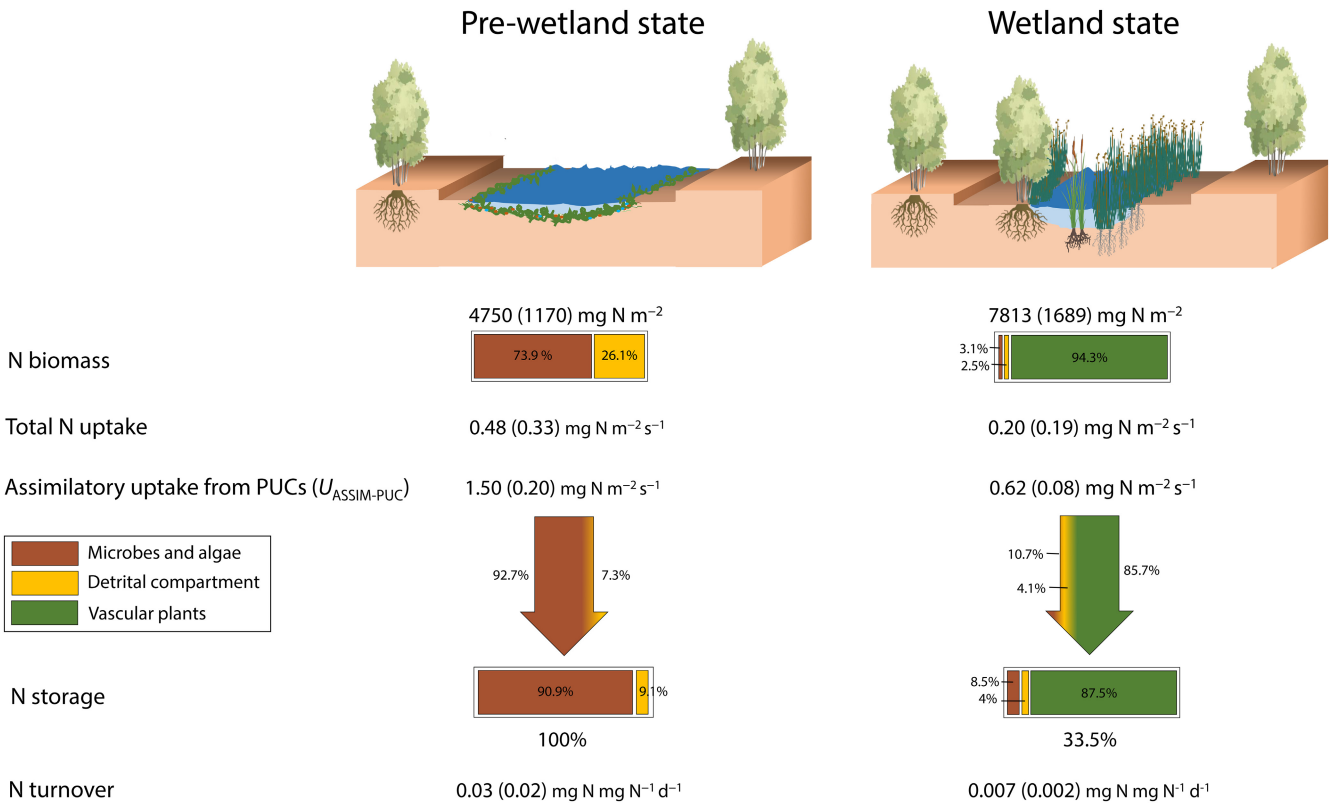

Fig. 5. Summary of N uptake, storage and turnover in the pre-wetland and wetland reaches. Percentages in boxes reflect the relative contribution of each PUC class to reach-scaled N biomass (above) and the ^{15}N storage into biomass (below). Percentages in vertical arrows reflect the relative contribution of each PUC class to assimilatory NH_4^+ uptake from ^{15}N tracer into biomass ($U_{ASSIM-PUC}$). N storage percentage refers to the total ^{15}N retained in biomass with respect to total added. Uncertainty for each parameter is shown in brackets as the standard deviation calculated based on the Monte Carlo method (see main text for details).

communities on streambed sediments (i.e., periphyton) and detritus (i.e., FBOM). The reach in the wetland state was characterized by a dominance of emergent vascular plants and riparian trees and shrubs, a result of cattle cessation along the stream-riparian corridor (Heffernan 2008; Heffernan et al. 2008). Based on the characteristics of the dominant primary producers, we expected significant differences in whole-stream metabolic activity and thus, in the N uptake between the two ecosystem states. Since vascular plants tend to have higher biomass and nutrient and energy requirements, and longer lifespan than filamentous green algae or diatoms, we predicted a lower N uptake demand and N storage capacity but a higher turnover rate in the pre-wetland state than in the wetland state.

Results only partially matched our predictions. Measured S_w and V_f in the two states (Table 2) were in the high range of stream values in terms of N uptake efficiency (i.e., short S_w values) and N demand (i.e., high V_f values) of streams elsewhere, which is expected for N-limited streams (Ensign and Doyle 2006; Ribot et al. 2017). Nevertheless, S_w was threefold shorter and V_f was one order of magnitude higher in the pre-wetland state than in the wetland state (Table 2). These results indicate that in-stream efficiency of N retention is higher in the pre-wetland state than in the wetland state. Unexpectedly, we observed that areal N uptake (i.e., U) and storage in the pre-wetland state were both higher than in the wetland state (Table 2). Interestingly, a previous study conducted in the same stream in the 80s (i.e., pre-wetland state) showed that the N storage capacity can be even higher than that measured in our study (Grimm 1987). Nonetheless, according to our predictions, the turnover rate in the pre-wetland state was lower than in the wetland state. Altogether, our results indicate that the two ecosystem states cycled N efficiently, but through different biogeochemical pathways. Higher N uptake and turnover indicates fast in-stream N cycling in the pre-wetland state, whereas both lower N uptake and N turnover indicates that in-stream N cycling is slowed down in the wetland state and that it was mostly characterized by more persistent N retention in vascular plants (as summarized in Fig. 5).

There are several mechanisms that may explain observed differences in U between the two stream ecosystem states. Reach-scale NH_4^+ uptake is mainly driven by nitrification and assimilatory uptake in streams (Peterson et al. 2001; Ribot et al. 2017). Nitrification, the aerobic oxidation of NH_4^+ to

NO_3^- carried by some specialized microbes, can comprise a substantial portion of NH_4^+ uptake in some streams (Peterson et al. 2001; Ribot et al. 2017). However, we observed a low contribution of nitrification to U (≤ 25%) in the two study stream reaches, especially in the wetland state (Table 2). Low nitrification rates may be explained by the high light availability reaching the stream channel (for pre-wetland only) which can inhibit nitrifiers (Merbt et al. 2012) or because photoautotrophic and heterotrophic microorganisms outcompete nitrifiers for NH_4^+ under high environmental C : N ratios such as those expected in an N-limited stream (Verhagen and Laanbroek 1991; Strauss and Lamberti 2000).

In streams, it is common that assimilatory uptake accounts for the largest fraction of U (Peterson et al. 2001; Ribot et al. 2017; Tank et al. 2018). Our results support these previous findings (Table 2). However, it is worth noting that assimilatory uptake estimated from the sum of PUC-specific uptakes ($U_{ASSIM-PUC}$) was considerably higher than that estimated from N uptake in the water column ($U_{ASSIM-WATER}$) in both study reaches. This result highlights the importance of primary producers in N cycling in this N-limited, open-channel stream. Nevertheless, the mismatch between the U_{ASSIM} estimates may be potentially explained by two methodological issues: (1) the most active parts of each PUC (i.e., hotspots of NH_4^+ uptake) were sampled disproportionately compared to other parts of these compartments (Peipoch et al. 2016); or (2) the spike added in water samples to bring the N mass to the minimum required for the mass spectrometric analysis may have underestimated ^{15}N in the water. Dilution of ^{15}N signal in the sample may result in an underestimation of the $^{15}NH_4^+$, with a minor effect on water-column estimations (i.e., based on the slope of longitudinal ^{15}N fluxes) but a greater impact on water-to-PUC ^{15}N ratio used to calculate assimilatory uptake. Alternatively, reach-scale biogeochemical processes that may counterbalance NH_4^+ uptake, such as mineralization, may lead to an underestimate of U from declines in water column fluxes of NH_4^+ along the reaches (Tank et al. 2018). In spite of this, the observation that U was mostly driven by assimilatory uptake suggests that differences in N cycling between the two ecosystem states are likely related to the intrinsic metabolic and structural characteristics of the dominant PUCs, in this case, primary producers.

Assimilatory N uptake by the most abundant PUCs in the pre-wetland state (i.e., *C. glomerata*, Zygnematales and periphyton) was clearly higher than assimilation by PUCs in the wetland state (i.e., vascular plants) (Fig. 2B). Furthermore, vascular plants showed lower N turnover rates; findings that align with the general trends observed at the reach scale (Fig. 4). These results may mechanistically explain the observed reach-scale differences in N cycling. In addition, establishment of vascular plants in the stream channel can also indirectly contribute to lower reach-scale N uptake by reducing the water exchange between the surface stream and the hyporheic zone, as reported in Heffernan et al. (2008). Similarly, Dong et al. (2017) observed that restriction of surface–subsurface water exchange was likely a major effect of the ecosystem state change to wetland dominance that influenced longitudinal patterns of stream nutrient concentration. The hyporheic zone is considered a relevant in-stream compartment of N uptake (Jones et al. 1995; Hall et al. 2002); thus, reducing the water exchange with this bioreactive zone may decrease reach-scale N uptake. Nevertheless, both bromide concentrations and $\delta^{15}NH_4^+$ measured at 20, 45, and 60 m downstream of the addition point during the tracer solute additions in the wetland reach were very similar in surface and subsurface samples (mean ± SE = 0.69 ± 0.009 and 0.69 ± 0.009 mg L^{-1} Br and 90.7 ± 14.1 and 83.9 ± 15.3 $\delta^{15}NH_4^+$, respectively), which indicates that there was vertical hydrological exchange to some extent. We also observed a disproportionate contribution of *S. goodingii* roots to N uptake with respect to their N biomass, in comparison to the aboveground biomass of *S. americanus* or *T. domingensis* (Fig. 2A,B). These results suggest that the presence of riparian vegetation may substantially contribute to in-stream N uptake in the wetland state. This is in agreement with the findings observed in the pre-wetland state that show the relevance of riparian trees for N retention in this stream (Schade et al. 2005).

We also found that the shift from algae to vascular plants as dominant primary producers in the study stream may not only affect reach-scale N uptake, but also the time that the assimilated N is stored in biomass before it is released back to the water column as inorganic N (i.e., reach-scale N turnover) (Table 2). In general, vascular plants live longer than diatoms and filamentous green algae, causing lower N turnover rates in the former than in the latter (Peipoch et al. 2014). The lower N turnover rate in vascular plants may explain why temporary N retention in wetland state biomass was four times longer when compared to the pre-wetland state reach (i.e., 142 and 33 d, respectively). Differences between states in the time over which N is immobilized in biomass may have important implications for N export from the watershed, especially considering the hydrologic regime of desert streams, which is characterized by extreme events. The frequent and severe flash floods and extended dry periods (Fisher et al. 1982; Stanley et al. 1997; Bunn et al. 2006) may affect the capacity of N retention in the two ecosystem states differently. Floods easily mobilize organic material grown and stored in the streambed sediments, resulting in high N export to downstream reaches (Grimm and Fisher 1989). Nevertheless, previous studies indicate that primary producers in desert streams under pre-wetland state conditions are highly resilient, and rapidly recover their biomass and nutrient uptake capacity after floods (Grimm and Fisher 1989; Marti et al. 1997). Wetland vascular plants, on the other hand, may be better adapted to withstand floods than filamentous algae and biofilm, due to their anchored root systems (Lytle and Poff 2004; Zhu et al. 2012). Furthermore, streambed establishment of vascular plants produces a suite of additional changes that reinforce their

stability (Dent et al. 2002; Heffernan 2008). Therefore, higher resistance of vascular plants to floods in the wetland state may result in lower export of assimilated N to downstream reaches in desert streams during storm events. On the other hand, the specific plant location of stored N within each vascular plant species may also have consequences for N export during storms and plant senescence (i.e., loss of aboveground biomass at the end of the reproductive period) (Fig. 3; Vernescu et al. 2005).

In conclusion, our results indicate that the two alternative stream ecosystem states, characterized by different primary producers, cycle N differently in the study stream (Fig. 5). More specifically, we showed that N spiraling in this N-limited stream changed from a dominance of intense and fast recycling to a prevalence of N retention in biomass of primary producers. The pre-wetland state, dominated by diatoms and filamentous green algae, shows higher capacity to take up and store N than the wetland state, which was dominated by emergent vascular plants (Fig. 2). However, the wetland state showed lower turnover rates, indicating that assimilated N is retained in the stream for longer time as organic N in biomass (Fig. 4). These reach-scale contrasting patterns are mostly explained by the differences in assimilatory uptake by the dominant primary producers present in each stream state and the environmental hydromorphological changes that they determine or induce. Differences in N cycling between ecosystem states may have further implications within the context of the highly variable hydrologic regime of desert streams (i.e., alternation of floods and dry events). Establishment of vascular plants in the wetland lowered N uptake capacity with respect to algal dominance in the pre-wetland state; however, higher resistance by vascular plants to episodic high floods and drying may result in a more stable N uptake over a wider range of flow conditions vs. a more cyclic and variable behavior in the pre-wetland state. In addition, the wetland state may reduce downstream N export during high-flow conditions due to the higher temporal N retention in biomass.

References

Allen, A. P., J. F. Gillooly, and J. H. Brown. 2005. Linking the global carbon cycle to individual metabolism. Funct. Ecol. **19**: 202–213. doi:10.1111/j.1365-2435.2005.00952.x

APHA. 1995. WPCF, standard methods for the examination of water and wastewater. American Public Health Association, American Water Works Association, Water Environment Federation.

Boada, J., and others. 2017. Immanent conditions determine imminent collapses: Nutrient regimes define the resilience of macroalgal communities. Proc. R. Soc. B Biol. Sci. **284**: 20162814. doi:10.1098/rspb.2016.2814

Brighenti, S., M. Tolotti, M. C. Bruno, G. Wharton, M. T. Pusch, and W. Bertoldi. 2019. Ecosystem shifts in Alpine streams under glacier retreat and rock glacier thaw: A review. Sci. Total Environ. **675**: 542–559. doi:10.1016/J.SCITOTENV.2019.04.221

Bunn, S. E., M. C. Thoms, S. K. Hamilton, and S. J. Capon. 2006. Flow variability in dryland rivers: Boom, bust and the bits in between. River Res. Appl. **22**: 179–186. doi:10.1002/rra.904

Busch, D. E., and S. G. Fisher. 1981. Metabolism of a desert stream. Freshw. Biol. **11**: 301–307. doi:10.1111/j.1365-2427.1981.tb01263.x

Conversi, A., and others. 2015. A holistic view of marine regime shifts. Philos. Trans. R. Soc. Biol. Sci. **370**: 20130279.

Dent, C. L., G. S. Cumming, and S. R. Carpenter. 2002. Multiple states in river and lake ecosystems. Philos. Trans. R. Soc. Lond. Ser. B Biol. Sci. **357**: 635–645. doi:10.1098/rstb.2001.0991

Dodds, W. K., and others. 2004. Carbon and nitrogen stoichiometry and nitrogen cycling rates in streams. Oecologia **140**: 458–467. doi:10.1007/s00442-004-1599-y

Dong, X., N. B. Grimm, J. B. Heffernan, and R. Muneepeerakul. 2019. Interactions between physical template and self-organization shape plant dynamics in a stream ecosystem. Ecosystems **23**: 891–905. doi:10.1007/s10021-019-00444-z

Dong, X., N. B. Grimm, K. Ogle, and J. Franklin. 2016. Temporal variability in hydrology modifies the influence of geomorphology on wetland distribution along a desert stream. J. Ecol. **104**: 18–30. doi:10.1111/1365-2745.12450

Dong, X., A. Ruhí, and N. B. Grimm. 2017. Evidence for self-organization in determining spatial patterns of stream nutrients, despite primacy of the geomorphic template. Proc. Natl. Acad. Sci. USA **114**: E4744–E4752. doi:10.1073/pnas.1617571114

Drummond, J. D., S. Bernal, D. von Schiller, and E. Martí. 2016. Linking in-stream nutrient uptake to hydrologic retention in two headwater streams. Freshw. Sci. **35**: 1176–1188.

Dudley, T. L., and N. B. Grimm. 1994. Modification of macrophyte resistance to disturbance by an exotic grass, and implications for desert stream succession, p. 1456–1460. *In* A. Sladeckova [ed.], Proc. Int. Assoc. Theoretical Appl. Limnol., Vol **25**.

Dutton, C. L., A. L. Subalusky, S. K. Hamilton, E. C. Bayer, L. Njoroge, E. J. Rosi, and D. M. Post. 2021. Alternative biogeochemical states of river pools mediated by hippo use and flow variability. Ecosystems **24**: 284–300. doi:10.1007/s10021-020-00518-3

Ensign, S. H., and M. W. Doyle. 2006. Nutrient spiraling in streams and river networks. J. Geophys. Res. **111**: G04009. doi:10.1029/2005jg000114

Fisher, S. G., L. J. Gray, N. B. Grimm, and D. E. Busch. 1982. Temporal succession in a desert stream ecosystem following flash flooding. Ecol. Monogr. **52**: 93–110. doi:10.2307/2937346

Gordon, N. D., T. A. McMahon, and B. L. Finlayson. 2004. Stream hydrology: An introduction for ecologists. John Wiley and Sons.

Grimm, N. B. 1987. Nitrogen dynamics during succession in a desert stream. Ecology **68**: 1157–1170.

Grimm, N. B., and S. G. Fisher. 1986. Nitrogen limitation in a Sonoran Desert stream. J. N. Am. Benthol. Soc. **5**: 2–15.

Grimm, N. B., and S. G. Fisher. 1989. Stability of periphyton and macroinvertebrates to disturbance by flash floods in a desert stream. J. N. Am. Benthol. Soc. **8**: 293–307. doi:10.2307/1467493

Hall, R. O., E. S. Bernhardt, and G. E. Likens. 2002. Relating nutrient uptake with transient storage in forested mountain streams. Limnol. Oceanogr. **47**: 255–265.

Hall, R. O., and E. R. Hotchkiss. 2017. Stream metabolism, p. 219–233. *In* Methods in stream ecology: Third edition. Elsevier.

Heffernan, J. B. 2008. Wetlands as an alternative stable state in desert streams. Ecology **89**: 1261–1271. doi:10.1890/07-0915.1

Heffernan, J. B., R. A. Sponseller, and S. G. Fisher. 2008. Consequences of a biogeomorphic regime shift for the hyporheic zone of a Sonoran Desert stream. Freshw. Biol. **53**: 1954–1968. doi:10.1111/j.1365-2427.2008.02019.x

Holmes, R. M., J. W. McClelland, D. M. Sigman, B. Fry, and B. J. Peterson. 1998. Measuring N-15-NH4+ in marine, estuarine and fresh waters: An adaptation of the ammonia diffusion method for samples with low ammonium concentrations. Mar. Chem. **60**: 235–243.

Ibáñez, C., and others. 2012. Regime shift from phytoplankton to macrophyte dominance in a large river: Top-down versus bottom-up effects. Sci. Total Environ. **416**: 314–322. doi:10.1016/j.scitotenv.2011.11.059

Jones, J. B., S. G. Fisher, and N. B. Grimm. 1995. Nitrification in the Hyporheic zone of a desert stream ecosystem. J. N. Am. Benthol. Soc. **14**: 249–258. doi:10.2307/1467777

Kearney, M. A., and W. Zhu. 2012. Growth of three wetland plant species under single and multi-pollutant wastewater conditions. Ecol. Eng. **47**: 214–220. doi:10.1016/j.ecoleng.2012.06.014

Kosinski, R. J. 1984. A comparison of the accuracy and precision of several open-water oxygen productivity techniques. Hydrobiologia **119**: 139–148.

Law, A., F. McLean, and N. J. Willby. 2016. Habitat engineering by beaver benefits aquatic biodiversity and ecosystem processes in agricultural streams. Freshw. Biol. **61**: 486–499. doi:10.1111/FWB.12721

Levi, P. S., T. Riis, A. B. Alnøe, M. Peipoch, K. Maetzke, C. Bruus, and A. Baattrup-Pedersen. 2015. Macrophyte complexity controls nutrient uptake in lowland streams. Ecosystems **18**: 914–931.

Lytle, D. A., and N. L. Poff. 2004. Adaptation to natural flow regimes. Trends Ecol. Evol. **19**: 94–100. doi:10.1016/j.tree.2003.10.002

Marti, E., N. B. Grimm, and S. G. Fisher. 1997. Pre- and post-flood retention efficiency of nitrogen in a Sonoran Desert stream. J. N. Am. Benthol. Soc. **16**: 805–819. doi:10.2307/1468173

McGowan, S., P. R. Leavitt, R. I. Hall, N. J. Anderson, E. Jeppesen, and B. V. Odgaard. 2005. Controls of algal abundance and community composition during ecosystem state change. Ecology **86**: 2200–2211. doi:10.1890/04-1029

Merbt, S. N., D. A. Stahl, E. O. Casamayor, E. Marti, G. W. Nicol, and J. I. Prosser. 2012. Differential photoinhibition of bacterial and archaeal ammonia oxidation. FEMS Microbiol. Lett. **327**: 41–46. doi:10.1111/j.1574-6968.2011.02457.x

Moore, J. W. 2006. Animal ecosystem engineers in streams. Bioscience **56**: 237–246 doi:10.1641/0006-3568(2006)056[0237:AEEIS]2.0.CO;2

Mulholland, P. J., J. L. Tank, D. M. Sanzone, W. M. Wollheim, B. J. Peterson, J. R. Webster, and J. L. Meyer. 2000. Nitrogen cycling in a forest stream determined by a N-15 tracer addition. Ecol. Monogr. **70**: 471–493 doi:10.1890/0012-9615(2000)070[0471:nciafs]2.0.co;2

Nikolakopoulou, M., A. Argerich, J. D. Drummond, E. Gacia, E. Martí, A. Sorolla, and F. Sabater. 2018. Emergent macrophyte root architecture controls subsurface solute transport. Water Resour. Res. **54**: 5958–5972.

Peipoch, M., E. Gacia, E. Bastias, A. Serra, L. Proia, M. Ribot, S. N. Merbt, and E. Marti. 2016. Small-scale heterogeneity of microbial N uptake in streams and its implications at the ecosystem level. Ecology **97**: 1329–1344. doi:10.1890/15-1210.1

Peipoch, M., E. Gacia, A. Pastor, M. Ribot, J. L. Riera, F. Sabater, and E. Martí. 2014. Intrinsic and extrinsic drivers of autotrophic nitrogen cycling in stream ecosystems: Results from a translocation experiment. Limnol. Oceanogr. **59**: 1973–1986. doi:10.4319/lo.2014.59.6.1973

Peterson, B. J., and others. 2001. Control of nitrogen export from watersheds by headwater streams. Science (80-) **292**: 86–90.

Peterson, C. G., and N. B. Grimm. 1992. Temporal variation in enrichment effects during periphyton succession in a nitrogen-limited desert stream ecosystem. J. N. Am. Benthol. Soc. **11**: 20–36. doi:10.2307/1467879

R Core Team. (2018). R: A language and environment for statistical computing. Vienna, Austria: R Foundation for Statistical Computing. Retrieved from https://cran.r-project.org/

Ribot, M., D. von Schiller, and E. Martí. 2017. Understanding pathways of dissimilatory and assimilatory dissolved inorganic nitrogen uptake in streams. Limnol. Oceanogr. **62**: 1166–1183. doi:10.1002/lno.10493

Riis, T., and others. 2019. Riverine macrophytes control seasonal nutrient uptake via both physical and biological pathways. Freshw. Biol. **65**: 178–192. doi:10.1111/fwb.13412

Salehin, M., A. I. Packman, and A. Wörman. 2003. Comparison of transient storage in vegetated and unvegetated

reaches of a small agricultural stream in Sweden: Seasonal variation and anthropogenic manipulation. Adv. Water Resour. **26**: 951–964. doi:10.1016/S0309-1708(03)00084-8

Schade, J. D., J. R. Welter, E. Marti, and N. B. Grimm. 2005. Hydrologic exchange and N uptake by riparian vegetation in an arid-land stream. J. N. Am. Benthol. Soc. **24**: 19–28 doi:10.1899/0887-3593(2005)024<0019:heanub>2.0.co;2

Scheffer, M., S. Carpenter, J. A. Foley, C. Folke, and B. Walker. 2001. Catastrophic shifts in ecosystems. Nature **413**: 591–596. doi:10.1038/35098000

Sigman, D. M., M. A. Altabet, R. Michener, D. C. McCorkle, B. Fry, and R. M. Holmes. 1997. Natural abundance-level measurement of the nitrogen isotopic composition of oceanic nitrate: An adaptation of the ammonia diffusion method. Mar. Chem. **57**: 227–242.

Solórzano, L. 1969. Determination of ammonia in natural waters by the phenolhypochlorite method 1 1 This research was fully supported by U.S. Atomic Energy Commission Contract No. ATS (11-1) GEN 10, P.A. 20. Limnol. Oceanogr. **14**: 799–801. doi:10.4319/lo.1969.14.5.0799

Stanley, E. H., S. G. Fisher, and N. B. Grimm. 1997. Ecosystem expansion and contraction in streams. Bioscience **47**: 427–435. doi:10.2307/1313058

Steffen, W., and others. 2011. The anthropocene: From global change to planetary stewardship. Ambio **40**: 739–761. doi:10.1007/s13280-011-0185-x

Strauss, E. A., and G. A. Lamberti. 2000. Regulation of nitrification in aquatic sediments by organic carbon. Limnol. Oceanogr. **45**: 1854–1859.

Stream Solute Workshop. 1990. Concepts and methods for assessing solute dynamics in stream ecosystems. J. N. Am. Benthol. Soc. **9**: 95–119. doi:10.2307/1467445

Svengsouk, L. J., and W. J. Mitsch. 2001. Dynamics of mixtures of typha latifolia and *Schoenoplectus tabernaemontani* in nutrient-enrichment wetland experiments. Am. Midl. Nat. **145**: 309–324 doi:10.1674/0003-0031(2001)145[0309:DOMOTL]2.0.CO;2

Tank, J. L., and others. 2018. Partitioning assimilatory nitrogen uptake in streams: An analysis of stable isotope tracer additions across continents. Ecol. Monogr. **88**: 120–138. doi:10.1002/ecm.1280

Twilley, R. R., L. R. Blanton, M. M. Brinson, and G. J. Davis. 1985. Biomass production and nutrient cycling in aquatic macrophyte communities of the Chowan River, North Carolina. Aquat. Bot. **22**: 231–252. doi:10.1016/0304-3770(85)90002-6

Verhagen, F. J. M., and H. J. Laanbroek. 1991. Competition for ammonium between nitrifying and heterotrophic bacteria in dual energy-limited chemostats. Appl. Environ. Microbiol. **57**: 3255–3263. doi:10.1128/aem.57.11.3255-3263.1991

Vernescu, C., J. Coulas, and P. Ryser. 2005. Leaf mass loss in wetland graminoids during senescence. Oikos **109**: 187–195. doi:10.1111/j.0030-1299.2005.13511.x

Weller, N. A., D. L. Childers, L. Turnbull, and R. F. Upham. 2016. Aridland constructed treatment wetlands I: Macrophyte productivity, community composition, and nitrogen uptake. Ecol. Eng. **97**: 649–657. doi:10.1016/j.ecoleng.2015.05.044

Wollheim, W. M., T. K. Harms, B. J. Peterson, K. Morkeski, C. S. Hopkinson, R. J. Stewart, M. N. Gooseff, and M. A. Briggs. 2014. Nitrate uptake dynamics of surface transient storage in stream channels and fluvial wetlands. Biogeochemistry **120**: 239–257. doi:10.1007/s10533-014-9993-y

Zhu, G., W. Li, M. Zhang, L. Ni, and S. Wang. 2012. Adaptation of submerged macrophytes to both water depth and flood intensity as revealed by their mechanical resistance. Hydrobiologia **696**: 77–93. doi:10.1007/s10750-012-1185-y

Acknowledgments

We thank all the LINX I fellows for development of field procedures and data analysis and inspirational discussions on these issues. We also thank the ASU stream group, Jen Tank and Jeremiah McGehee, Erin Worth, Truman Combs, Emma Holland, Marena Sampson, Alex Meyr, Rebecca Hale, and Xiaoli Dong for assistance in the field and in the lab. This work was supported by the US NSF LTREB program, grant DEB-145722. Miquel Ribot's stage at Grimm's lab was supported by the BE fellowship from Generalitat de Catalunya (ref: 2012 BE1 00379). Daniel von Schiller is a Serra Húnter Fellow.

Conflict of Interest

None declared.

Submitted 16 January 2021
Revised 29 October 2021
Accepted 14 March 2022

Associate editor: Edward G. Stets